Nonlinear Analysis: Hybrid Systems 23 (2017) 1–10

Contents lists available at ScienceDirect

Nonlinear Analysis: Hybrid Systems

journal homepage: www.elsevier.com/locate/nahs

Edge agreement of second-order multi-agent system with dynamic quantization via the directed edge Laplacian

Zhiwen Zeng [a], Xiangke Wang [a,*], Zhiqiang Zheng [a], Lina Zhao [b]

[a] College of Mechanics and Automation, National University of Defense Technology, Changsha, Hunan, China
[b] Inner Mongolia Agricultural University, Hohhot, Inner Mongolia, China

ARTICLE INFO

Article history:
Received 29 August 2015
Accepted 20 May 2016
Available online 27 June 2016

Keywords:
Edge agreement
Edge Laplacian
Model reduction
Dynamic quantization

ABSTRACT

This work explores the edge agreement problem of second-order multi-agent systems with dynamic quantization under directed communication. To begin with, by virtue of the directed edge Laplacian, we propose a model reduction representation of the closed-loop multi-agent system depending on the spanning tree subgraph. Considering the limitations of the finite bandwidth channels, the quantization effects of second-order multi-agent systems under directed graph are considered. The static quantizers generally contain a fixed quantization interval and infinite quantization level, which are, to some extent, inefficient and impractical. To further reduce the bit depth (number of bits available) and to obtain better precision, the dynamic quantized communication strategy referring to zooming in-zooming out scheme is required. Based on the reduced model associated with the *essential edge Laplacian*, the asymptotic stability of second-order multi-agent systems under dynamic quantized effects with only finite quantization level can be guaranteed. Finally, the simulation of altitude alignment of micro air vehicles is provided to verify the theoretical results.

1. Introduction

The coordination control problem of multi-agent systems has received increasing amounts of attention recently. Network topology and information flow have turned out to be an important concern of such issue, as the constraints on communication have a considerable impact on the performance of multi-agent systems. Early efforts on such problem primarily focused on the assumption that agents can obtain precise information through local communication as in [1,2]. However, in practical, only a finite amount of information data can be transmitted among neighbors at each time instant, since the digital channels are always subjected to a limited channel capacity.

To cope with the limitations of the finite bandwidth channels, information data are generally processed by quantizers. The spectral properties of the incidence matrix is employed to carry out the convergence analysis of multi-agent systems for both uniform quantizer and logarithmic quantizer in [3]. Further, in [4], by using stochastic gossiping algorithm, the explicit relationship between the convergence rate and the communication topology is revealed for uniform quantizers. Note that, the above-mentioned static quantizers require infinite quantization level which is impractical; and the fixed quantization interval always leads to practical stability rather than asymptotic stability. Therefore, the dynamic quantizer with finite quantization level is more of practical significance. In [5], the coding/decoding strategies based on zooming in-zooming

* Corresponding author.
E-mail address: xkwang@nudt.edu.cn (X. Wang).

http://dx.doi.org/10.1016/j.nahs.2016.05.006
1751-570X/

out scheme for dynamic uniform quantizer are proposed to maintain average consensus. Based on dynamic encoding and decoding scheme, [6] provides an explicit relationship of the asymptotic convergence and the network parameters, especially, the quantization level. In addition, the authors of [6] also provide a way to reduce the number of transmitting bits along each digital channel down to merely one bit. Most recently, extensions of [6] are further discussed in view of the quantized consensus over directed networks [7–9]. Note that, these methods are mainly devised for first-order multi-agent systems. Nevertheless, these methods may lead to a dramatically different coordination behavior while considering second-order dynamics, even though the agents are coupled through similar network topology [10]. To the best of authors' knowledge, there are still little works to explore the dynamic quantization effects on second-order dynamics. [11] proposes a quantized-observer based encoding–decoding scheme for second-order multi-agent systems with limited information, which shows that exponential asymptotic synchronization can be achieved with 2-bit quantizer for connected graph. The zooming in-zooming out strategy is proposed to achieve asymptotic average consensus for double-integrator multi-agent systems with dynamically quantized information transmission in [12]. However, the above-mentioned literatures only consider the quantization effects associated with undirected graph. Since the quantization may cause undesirable oscillating behavior under directed topology [13], the scenario considering directed graph is still very challenging.

In this paper, we are going to extend our previous work of [14] to deal with the challenging scenario that second-order multi-agent systems with dynamic quantization under directed graph. Note that the analysis of the node agreement (consensus problem) has matured, but the work related to the edge agreement [15,16] has not been deeply studied yet. Since quantized measurements bring enormous challenges to the analysis of the synchronization behavior of the second-order multi-agent systems, we are going to explore more details about this term by virtue of the reduced edge agreement model. The main contributions of this paper contain three aspects. First, a model reduction representation of the closed-loop multi-agent system is derived based on the observation that the co-spanning tree subsystem can be served as an internal feedback. By utilizing the reduced edge agreement model, the analysis of the whole system can be extremely simplified. Second, contrary to [11] and [12], the challenging scenario that second-order multi-agent systems with dynamic quantization under directed graph is considered. Third, by using the zooming in-zooming out scheme, the asymptotic stability of second-order multi-agent systems under dynamic quantized effects can be guaranteed with only finite quantization level and the theoretic results are verified by achieving altitude alignment of micro air vehicles.

The rest of the paper is organized as follows: preliminaries and some related notions are proposed in Section 2. The dynamic quantized edge agreement with second-order multi-agent systems under directed graph is studied in Section 3. The simulation results are provided in Section 4, while the last section draws the conclusion.

2. Basic notions and preliminary results

In this section, some basic notions in graph theory and preliminary results about the synchronization of multi-agent systems under quantized information are briefly introduced.

2.1. Graph and matrix

In this paper, we use $|\cdot|$ and $\|\cdot\|$ to denote the Euclidean norm and 2-norm for vectors and matrices, respectively. Denote by I_n the identity matrix and by $\mathbf{0}_n$ the zero matrix in $\mathbb{R}^{n\times n}$. Let $\mathbf{0}$ be the column vector with all zero entries. Let $\mathcal{G} = (\mathcal{V}, \mathcal{E})$ be a digraph of order N specified by a node set $\mathcal{V}$ and an edge set $\mathcal{E} \subseteq \mathcal{V} \times \mathcal{V}$ with size L. The set of neighbors of node i is denoted by $\mathcal{N}_i = \{j : e_k = (j, i) \in \mathcal{E}\}$. The adjacency matrix of $\mathcal{G}$ is defined as $A_{\mathcal{G}} = \left[a_{ij}\right] \in \mathbb{R}^{N\times N}$ with nonnegative adjacency elements $a_{ij} > 0 \Leftrightarrow (j, i) \in \varepsilon$. The degree matrix $\Delta_{\mathcal{G}} = \left[\Delta_{ij}\right]$ is a diagonal matrix with $[\Delta_{ii}] = \sum_{j=1}^{N} a_{ij}$, $i = 1, 2, \ldots, N$, and the graph Laplacian of the weighted digraph $\mathcal{G}$ is defined by $L_{\mathcal{G}}(\mathcal{G}) = \Delta_{\mathcal{G}} - A_{\mathcal{G}}$ whose eigenvalues will be ordered and denoted as $0 = \lambda_0 = \cdots = \lambda_1 < \lambda_2 \leq \cdots \leq \lambda_N$. Denote by $\mathcal{W}(\mathcal{G})$ the $L \times L$ diagonal matrix of w_k, for $k = 1, 2, \ldots, L$, where w_k represents the weight of $e_k = (j, i) \in \mathcal{E}$. The incidence matrix $E(\mathcal{G})$ for a digraph is a $\{0, \pm 1\}$-matrix with rows and columns indexed by nodes and edges of $\mathcal{G}$, respectively, such that for edge $e_k = (j, i) \in \mathcal{E}$, $[E(\mathcal{G})]_{jk} = +1$, $[E(\mathcal{G})]_{ik} = -1$ and $[E(\mathcal{G})]_{lk} = 0$ for $l \neq i, j$. The in-incidence matrix $E_{\odot}(\mathcal{G}) \in \mathbb{R}^{N\times L}$ is a $\{0, -1\}$ matrix with rows and columns indexed by nodes and edges of $\mathcal{G}$, respectively, such that for an edge $e_k = (j, i) \in \mathcal{E}$, $[E_{\odot}(\mathcal{G})]_{lk} = -1$ for $l = i$, $[E_{\odot}(\mathcal{G})]_{lk} = 0$ otherwise. The weighted in-incidence matrix $E^{w}_{\odot}(\mathcal{G})$ can be defined as $E^{w}_{\odot}(\mathcal{G}) = E_{\odot}(\mathcal{G})\,\mathcal{W}(\mathcal{G})$. As thus, the graph Laplacian of $\mathcal{G}$ has the following expression [14]: $L_{\mathcal{G}}(\mathcal{G}) = E^{w}_{\odot}(\mathcal{G})E(\mathcal{G})^{T}$. The weighted edge Laplacian of a directed graph $\mathcal{G}$ can be defined as [14]

$$L_e(\mathcal{G}) := E(\mathcal{G})^{T}E^{w}_{\odot}(\mathcal{G}). \tag{1}$$

A directed path in digraph $\mathcal{G}$ is a sequence of directed edges and a directed tree is a digraph in which, for the root i and any other node j, there is exactly one directed path from i to j. A spanning tree $\mathcal{G}_{\mathcal{T}} = (\mathcal{V}, \mathcal{E}_1)$ of a directed graph $\mathcal{G} = (\mathcal{V}, \mathcal{E})$ is a directed tree formed by graph edges that connect all the nodes of the graph; a cospanning tree $\mathcal{G}_{\mathcal{C}} = (\mathcal{V}, \mathcal{E} - \mathcal{E}_1)$ of $\mathcal{G}_{\mathcal{T}}$ is the subgraph having all the vertices of $\mathcal{G}$ and exactly those edges that are not in $\mathcal{G}_{\mathcal{T}}$. Graph $\mathcal{G}$ is called *quasi-strongly connected* if and only if it has a directed spanning tree [17].

Lemma 1 ([14]). *For a quasi-strongly connected graph $\mathcal{G}$, the graph Laplacian $L_{\mathcal{G}}(\mathcal{G})$ and the edge Laplacian $L_e(\mathcal{G})$ have the same $N - 1$ nonzero eigenvalues, which are all in the open right-half plane.*

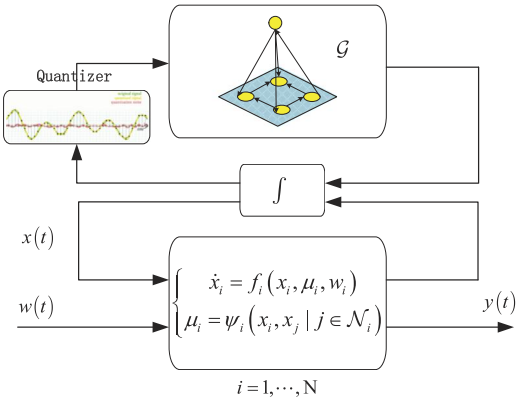

Fig. 1. The networked multi-agent system with the quantized states under topology $\mathcal{G}$.

Lemma 2 ([14]). *For a general quasi-strongly connected graph $\mathcal{G} = \mathcal{G}_\mathcal{T} \cup \mathcal{G}_\mathcal{C}$, $L_e(\mathcal{G})$ contains $L - N + 1$ zero eigenvalues. Moreover, if the edge set of $\mathcal{G}_\mathcal{C}$ is not empty, then zero is a simple root of the minimal polynomial of $L_e(\mathcal{G})$.*

2.2. Multi-agent system with dynamic uniform quantization

The dynamics of the isolated agent i is represented by

$$\dot{x}_i = f_i(x_i, \mu_i, w_i), \quad \text{for } i = 1, \ldots, n, \tag{2}$$

where $x_i \in \mathbb{R}^n$ and $\mu_i \in \mathbb{R}^n$ are the state and the control input, respectively, and $w_i \in \mathbb{R}^n$ is the disturbance if exists. In addition, the input μ_i $(i = 1, \ldots, n)$ is designed to achieve the coordinated objectives with the form of

$$\mu_i = h_i(x_i, x_j | j \in \mathcal{N}_i), \tag{3}$$

where $\mathcal{N}_i$ is the set of neighbors of agent i. As known, the coupling between each pair of networked agents can be characterized by the communication interconnection topology $\mathcal{G}$. To perform collective behaviors, the networked agents can be naturally modeled by graph $\mathcal{G}$ with vertices describing agents and the edges being the communication topology. Considering the limited capacity of the practical digital channels, the state values are always quantized, and only finite bits of information can be transmitted via network at each time instant. As thus, the networked multi-agent system with quantized states can be illustrated as the block diagram as shown in Fig. 1, in which the topology $\mathcal{G}$ is explicitly incorporated into the dynamical system as in [18].

To realize the quantized communication scheme, a dynamic encoder–decoder pair is employed. Particularly, the quantized information is encoded by the sender side before transmitting and dynamically decoded at the receiver side. Our purpose for this work mainly focuses on the *dynamic uniform quantization*. Suppose $\mathbb{L}$ is a finite subset of $\mathbb{R}$, then a dynamic uniform quantizer $q_\mu : \mathbb{R} \to \mathbb{L}$ is defined as

$$q_\mu(x_i) = \mu q_u\left(\frac{x_i}{\mu}\right) = \left(\left\lfloor \frac{x_i}{\mu\Delta} \right\rfloor + \frac{1}{2}\right)\mu\Delta \tag{4}$$

where q_u with quantization error Δ is a typical uniform quantizer as described in [13,14]; $\mu > 0$ is adopted as a zooming variable. For a finite-level uniform quantizer with the quantization range $\mathcal{M}$, we have $\left|q_\mu(x_i) - x_i\right| \le \mu\Delta$ if $|x_i| \le \mu\mathcal{M}$; and $\left|q_\mu(x_i)\right| = \mu(\mathcal{M} - \Delta/2)$, otherwise. For vector x, let $q_\mu(x) = \left[q_\mu(x_1), q_\mu(x_2), \ldots, q_\mu(x_N)\right]^T$. Then the following error bounds are hold: $\left|q_\mu(x) - x\right| \le \sqrt{N}\mu\Delta$, if $|x_i| \le \mu\mathcal{M}$; and $\left|q_\mu(x) - x\right| \le \sqrt{N}(\mathcal{M} - \Delta)$, if $|x_i| > \mu\mathcal{M}$. Suppose τ is a fixed positive number, the zooming variable μ will be updated at discrete time instants and maintain a constant value on each interval $(k\tau, k\tau + \tau]$, $k \in \mathbb{Z}_{\ge 0}$. As thus, the evolution of the networked multi-agent systems with time is discrete rather than continuous in most cases. In fact, by combining Eq. (4) with the given system (2) finally results in a *hybrid system*.

3. Quantized edge agreement under directed graph

Consider the quasi-strongly connected graph $\mathcal{G}$, the most commonly used consensus dynamics in [1] is described as $\dot{x} = -(L_g(\mathcal{G}) \otimes I_n)x$, where $\otimes$ denotes the Kronecker product. Contrary to the most existing works, we study the synchronization problem from the edge perspective by using $L_e(\mathcal{G})$. Following this way, we define the *edge state* vector as

$$x_e(t) = (E(\mathcal{G})^T \otimes I_n)x(t) \tag{5}$$

which represents the difference between the state components of two neighboring nodes. Taking the derivative of (5) leads to

$$\dot{x}_e(t) = -(L_e(\mathcal{G}) \otimes I_n)x_e(t) \tag{6}$$

which is referred to as *edge agreement dynamics* in this paper. In comparison to the node agreement (consensus), the edge agreement, rather than requiring the convergence to the agreement subspace, desires the edge agreement dynamics converge to the origin, i.e., $\lim_{t\to\infty} |x_e(t)| = 0$. Essentially, the evolution of an edge state depends on its current state and the states of its adjacent edges. In addition, the edge agreement implies consensus if the directed graph $\mathcal{G}$ has a spanning tree as mentioned in [16].

3.1. Reduced edge agreement model associated with a spanning tree

A quasi-strongly connected digraph $\mathcal{G}$ can be rewritten as a union form: $\mathcal{G} = \mathcal{G}_\mathcal{T} \cup \mathcal{G}_\mathcal{C}$. According to certain permutations, the incidence matrix $E(\mathcal{G})$ can always be rewritten as $E(\mathcal{G}) = \begin{bmatrix} E_\mathcal{T}(\mathcal{G}) & E_\mathcal{C}(\mathcal{G}) \end{bmatrix}$ as well. Since the cospanning tree edges can be constructed from the spanning tree edges via a linear transformation, such that $E_\mathcal{T}(\mathcal{G})\, T(\mathcal{G}) = E_\mathcal{C}(\mathcal{G})$ with $T(\mathcal{G}) = \left(E_\mathcal{T}(\mathcal{G})^T E_\mathcal{T}(\mathcal{G})\right)^{-1} E_\mathcal{T}(\mathcal{G})^T E_\mathcal{C}(\mathcal{G})$ and $rank(E(\mathcal{G})) = N - 1$ from [17]. Then we define

$$R(\mathcal{G}) = \begin{bmatrix} I & T(\mathcal{G}) \end{bmatrix} \tag{7}$$

and obtain $E(\mathcal{G}) = E_\mathcal{T}(\mathcal{G})\, R(\mathcal{G})$. The column space of $E(\mathcal{G})^T$ is known as the *cut space* of $\mathcal{G}$ and the null space of $E(\mathcal{G})$ is called as the *flow space*, which is the orthogonal complement of the cut space.

Before moving on, we introduce the following transformation matrix:

$$S_e(\mathcal{G}) = \begin{bmatrix} R(\mathcal{G})^T & \theta_e(\mathcal{G}) \end{bmatrix}$$

$$S_e(\mathcal{G})^{-1} = \begin{bmatrix} \left(R(\mathcal{G})\, R(\mathcal{G})^T\right)^{-1} R(\mathcal{G}) \\ \theta_e(\mathcal{G})^T \end{bmatrix}$$

where $\theta_e(\mathcal{G})$ denote the orthonormal basis of the flow space, i.e., $E(\mathcal{G})\,\theta_e(\mathcal{G}) = 0$. Since $rank(E(\mathcal{G})) = N-1$, one can obtain that $dim(\theta_e(\mathcal{G})) = \mathcal{N}(E(\mathcal{G}))$ and $\theta_e(\mathcal{G})^T \theta_e(\mathcal{G}) = I_{L-N+1}$.

Make use of the following transformation for (6):

$$S_e^{-1} x_e(t) = \begin{pmatrix} x_\mathcal{T}(t) \\ \mathbf{0} \end{pmatrix}$$

where $x_\mathcal{T} = E_\mathcal{T}(\mathcal{G})^T x(t)$ represents the states across a specific spanning tree. Then one can obtain a reduced model representation of (6) as follows:

$$\dot{x}_\mathcal{T} = -(E_\mathcal{T}(\mathcal{G})^T E^w_\odot(\mathcal{G}) R(\mathcal{G})^T \otimes I_n)x_\mathcal{T}(t) \tag{8}$$

which captures the dynamical behavior of the whole system. We refer $\hat{L}_e(\mathcal{G}) = E_\mathcal{T}(\mathcal{G})^T E^w_\odot(\mathcal{G}) R(\mathcal{G})^T$ as the *essential edge Laplacian*. Then we have the following lemma.

Lemma 3 ([14]). *The essential edge Laplacian $\hat{L}_e(\mathcal{G})$ has the same eigenvalues of $L_e(\mathcal{G})$ except the zero eigenvalues.*

It is clear that, by applying the above-mentioned similar transformation will lead to

$$S_e(\mathcal{G})^{-1} L_e(\mathcal{G}) S_e(\mathcal{G}) = \begin{bmatrix} \hat{L}_e(\mathcal{G}) & E^T_\mathcal{T}(\mathcal{G}) E^w_\odot(\mathcal{G}) \theta_e(\mathcal{G}) \\ \mathbf{0} & \mathbf{0} \end{bmatrix}. \tag{9}$$

Then the eigenvalues of the block matrix are the solution of

$$\lambda^{(L-N+1)} \det\left(\lambda I - \hat{L}_e(\mathcal{G})\right) = 0$$

which shows that $\hat{L}_e(\mathcal{G})$ has exactly all the nonzero eigenvalues of $L_e(\mathcal{G})$. Meanwhile, we can construct the following Lyapunov equation as

$$H\hat{L}_e(\mathcal{G}) + \hat{L}_e(\mathcal{G})^T H = -I_{N-1} \tag{10}$$

where H is a positive definite matrix.

As we have the partition that $\mathcal{G} = \mathcal{G}_\mathcal{T} \cup \mathcal{G}_\mathcal{C}$, the weighted in-incidence matrix can be represented as $E^w_\odot(\mathcal{G}) = \begin{bmatrix} E^w_{\odot_\mathcal{T}}(\mathcal{G}) & E^w_{\odot_\mathcal{C}}(\mathcal{G}) \end{bmatrix}$. From (8), one can obtain

$$\dot{x}_\mathcal{T}(t) = \left(-L^\mathcal{T}_e(\mathcal{G}) - E_\mathcal{T}(\mathcal{G})^T E^w_{\odot_\mathcal{C}}(\mathcal{G}) T(\mathcal{G})^T\right) \otimes I_n x_\mathcal{T}(t)$$

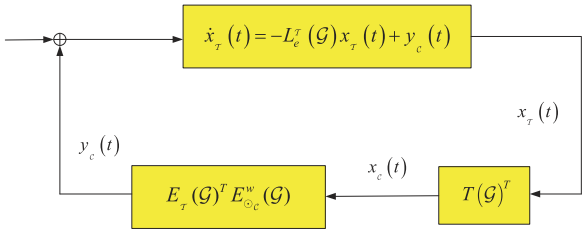

Fig. 2. The co-spanning tree states can serve as an internal feedback state.

where $L_e^{\mathcal{T}}(\mathcal{G}) = E_{\mathcal{T}}(\mathcal{G})^T E_{\odot_{\mathcal{T}}}^w(\mathcal{G})$. Since $E_{\mathcal{T}}(\mathcal{G})\,T(\mathcal{G}) = E_{\mathcal{C}}(\mathcal{G})$ as mentioned before, the co-spanning tree states can be reconstructed through the matrix $T(\mathcal{G})$ as

$$x_{\mathcal{C}} = \left(E_{\mathcal{C}}(\mathcal{G})^T \otimes I_n\right)x(t) = \left(T(\mathcal{G})\right)^T \otimes I_n)x_{\mathcal{T}}(t).$$

Therefore, the co-spanning tree states can be viewed as an internal feedback on the edges of the spanning tree subgraph shown in Fig. 2.

3.2. Main result and stability analysis

We consider a group of N networked agents. In view of that the second-order integrator dynamics can be a simple abstraction of a wide range of practical systems, so that the dynamics (2) of the ith agent is particularly given as

$$\begin{cases} \dot{x}_i(t) = v_i(t) \\ \dot{v}_i(t) = u_i(t) \end{cases} \tag{11}$$

where $x_i(t) \in \mathbb{R}^n$ is the position; $v_i(t) \in \mathbb{R}^n$ is the velocity; and $u_i(t) \in \mathbb{R}^n$ is the control input. The goal for designing distributed control law $u_i(t)$ is to synchronize the velocities and positions of the N-networked agents.

The generally studied second-order consensus protocol proposed in [10] is described as follows: $u_i(t) = \alpha \sum_{j\in\mathcal{N}_i}^N a_{ij}\left(x_j(t) - x_i(t)\right) + \beta \sum_{j\in\mathcal{N}_i}^N a_{ij}\left(v_j(t) - v_i(t)\right)$, for $i = 1, 2, \ldots, N$, where $\alpha > 0$ and $\beta > 0$ are the coupling strengths. As in [3], we assume that each agent i has only quantized measurements of the relative position $q_\mu\left(x_i - x_j\right)$ and velocity information $q_\mu\left(v_i - v_j\right)$. In that way, the protocol can be modified as

$$u_i(t) = \alpha \sum_{j\in\mathcal{N}_i}^N a_{ij} q_\mu\left(x_j(t) - x_i(t)\right) + \beta \sum_{j\in\mathcal{N}_i}^N a_{ij} q_\mu\left(v_j(t) - v_i(t)\right) \tag{12}$$

for $i = 1, 2, \ldots, N$.

To ease the notation, we simply use E, $E_{\odot}^w$ and L_e instead of $E(\mathcal{G})$, $E_{\odot}^w(\mathcal{G})$ and $L_e(\mathcal{G})$ in the following parts.

Considering the dynamics of the networked agents as describing in (11), by directly applying the quantized protocol (12), we obtain

$$\begin{cases} \dot{x}_i(t) = v_i(t) \\ \dot{v}_i(t) = \alpha \sum_{j\in\mathcal{N}_i}^N a_{ij} q_\mu\left(x_j(t) - x_i(t)\right) + \beta \sum_{j\in\mathcal{N}_i}^N a_{ij} q_\mu\left(v_j(t) - v_i(t)\right). \end{cases}$$

To ease the analysis, we technically choose $\alpha = \sigma^2$ and $\beta = \sigma^3\,(\sigma > 0)$ as in [19]. By using this trick, we can easily construct a positive definite matrix which helps us to simplify the proof of the main results. Then, the system can be collected as

$$\begin{cases} \dot{x}(t) = v(t) \\ \dot{v}(t) = -\sigma^2(E_{\odot}^w \otimes I_n)q_\mu\left((E^T \otimes I_n)x(t)\right) - \sigma^3(E_{\odot}^w \otimes I_n)q_\mu\left((E^T \otimes I_n)v(t)\right) \end{cases} \tag{13}$$

with $x(t)$, $v(t)$ denoting the column stack vector of $x_i(t)$ and $v_i(t)$, respectively.

By left-multiplying $E^T \otimes I_n$ of both sides of (13), we obtain

$$\begin{cases} \dot{x}_e = v_e \\ \dot{v}_e = -\sigma^2(L_e \otimes I_n)q_\mu(x_e) - \sigma^3(L_e \otimes I_n)q_\mu(v_e) \end{cases} \tag{14}$$

with $x_e = (E^T \otimes I_n)x$, $v_e = (E^T \otimes I_n)v$.

The quantization error satisfies $\left|e_{x_e}\right|, \left|e_{v_e}\right| \leq \sqrt{nL}\mu\Delta$, where $e_{x_e} = q_\mu\left(x_e\right) - x_e$ and $e_{v_e} = q_\mu\left(v_e\right) - v_e$. Then dynamic system (14) can be written as the following form:

$$\begin{cases} \dot{x}_e\left(t\right) = v_e\left(t\right) \\ \dot{v}_e\left(t\right) = -\sigma^2(L_e \otimes I_n)x_e - \sigma^3(L_e \otimes I_n)v_e - \sigma^2(L_e \otimes I_n)e_{x_e} - \sigma^3(L_e \otimes I_n)e_{v_e}. \end{cases} \tag{15}$$

Let $z = \begin{bmatrix} x_e^T & v_e^T \end{bmatrix}^T$ and $\omega = \begin{bmatrix} {e_{x_e}}^T & {e_{v_e}}^T \end{bmatrix}^T$, then system (15) can be recasted in a compact matrix form as follows:

$$\dot{z} = (\mathcal{L} \otimes I_n)z + (\mathcal{L}_1 \otimes I_n)\omega \tag{16}$$

with $\mathcal{L} = \begin{bmatrix} \mathbf{0}_L & I_L \\ -\sigma^2 L_e & -\sigma^3 L_e \end{bmatrix}$ and $\mathcal{L}_1 = \begin{bmatrix} \mathbf{0}_L & \mathbf{0}_L \\ -\sigma^2 L_e & -\sigma^3 L_e \end{bmatrix}$, where $|\omega| \leq \sqrt{2nL}\mu\Delta$.

Since L_e contains zero eigenvalues, the direct analysis of (16) is difficult. However, the reduced edge agreement model will be of great help in this scene. To begin with, we make use of the following transformation

$$S_e^{-1} \otimes I_n x_e = \begin{pmatrix} x_{\mathcal{T}} \\ \mathbf{0} \end{pmatrix} \qquad S_e^{-1} \otimes I_n v_e = \begin{pmatrix} v_{\mathcal{T}} \\ \mathbf{0} \end{pmatrix}$$

$$(S_e^{-1} \otimes I_n)e_{x_e} = \begin{bmatrix} \left(\left(RR^T\right)^{-1} R \otimes I_n\right)e_{x_e} \\ (\theta_e{}^T \otimes I_n)e_{x_e} \end{bmatrix}$$

$$(S_e^{-1} \otimes I_n)e_{v_e} = \begin{bmatrix} \left(\left(RR^T\right)^{-1} R \otimes I_n\right)e_{v_e} \\ (\theta_e{}^T \otimes I_n)e_{v_e} \end{bmatrix}.$$

Then we define $z_{\mathcal{T}} = \begin{bmatrix} x_{\mathcal{T}}^T & v_{\mathcal{T}}^T \end{bmatrix}^T$ and $\hat{L}_{\mathcal{O}} = E_{\mathcal{T}}^T E_{\odot}^w$. Finally, system (15) can be rewritten into

$$\dot{z}_{\mathcal{T}} = (\mathcal{L}_{\mathcal{T}} \otimes I_n)z_{\mathcal{T}} + (\mathcal{L}_{\mathcal{T}1} \otimes I_n)\omega \tag{17}$$

with $\mathcal{L}_{\mathcal{T}} = \begin{bmatrix} \mathbf{0}_{N-1} & I_{N-1} \\ -\sigma^2\hat{L}_e & -\sigma^3\hat{L}_e \end{bmatrix}$, $\mathcal{L}_{\mathcal{T}1} = \begin{bmatrix} \mathbf{0}_{(N-1\times L)} & \mathbf{0}_{(N-1\times L)} \\ -\sigma^2\hat{L}_{\mathcal{O}} & -\sigma^3\hat{L}_{\mathcal{O}} \end{bmatrix}$.

To further explore the quantization effects on the edge agreement, we propose the following theorem.

Theorem 1. *Considering the quasi-strongly connected digraph $\mathcal{G}$ associated with the edge Laplacian L_e, suppose $\mathcal{Q} = -\left(\mathcal{P}\mathcal{L}_{\mathcal{T}} + \mathcal{L}_{\mathcal{T}}^T\mathcal{P}\right)$ with $\mathcal{P} = \begin{bmatrix} \sigma H & H \\ H & \sigma H \end{bmatrix}$, where H is obtained by (10). Assume that $\mathcal{M}$ is large enough compared to Δ, so that we have*

$$\sqrt{\frac{\lambda_{\min}\left(\mathcal{P}\right)}{\lambda_{\max}\left(\mathcal{P}\right)}}\mathcal{M} > 2\Delta \max\left\{1, \frac{\sqrt{2nL}\left\|\mathcal{P}\mathcal{L}_{\mathcal{T}1}\right\|}{\lambda_{\min}\left(\mathcal{Q}\right)}\right\}. \tag{18}$$

Then there exists a hybrid quantized feedback control policy (12) that makes the edge agreement of (17) asymptotically achieved.

Proof. By selecting $\sigma > 1$, it is clearly that $\mathcal{P}$ is positive definite. Besides, by definition, we obtain

$$\mathcal{Q} = -\left(\mathcal{P}\mathcal{L}_{\mathcal{T}} + \mathcal{L}_{\mathcal{T}}^T\mathcal{P}\right) = \begin{bmatrix} \sigma^2 I_{N-1} & \sigma^3 I_{N-1} - \sigma H \\ \sigma^3 I_{N-1} - \sigma H & \sigma^4 I_{N-1} - 2H \end{bmatrix}.$$

Let $\mathcal{Q} = \begin{bmatrix} \mathcal{Q}_1 & \mathcal{Q}_2 \\ \mathcal{Q}_2^T & \mathcal{Q}_3 \end{bmatrix}$ with $\mathcal{Q}_1 = \sigma^2 I_{N-1}$, $\mathcal{Q}_2 = \sigma^3 I_{N-1} - \sigma H$ and $\mathcal{Q}_3 = \sigma^4 I_{N-1} - 2H$. According to Schur complements theorem [10], by selecting

$$\sigma > \sqrt{\frac{\lambda_{\max}(H)}{2} + 1}$$

then we have $\mathcal{Q}_1 > 0$ and $\mathcal{Q}_3 - \mathcal{Q}_2^T{\mathcal{Q}_1}^{-1}\mathcal{Q}_2 = H\left(2\left(\sigma^2 - 1\right)I_{N-1} - H\right) > 0$, so that $\mathcal{Q}$ is positive definite.

For the edge Laplacian dynamics (17), we can choose the following Lyapunov function candidate:

$$V\left(z_{\mathcal{T}}\right) = z_{\mathcal{T}}^T(\mathcal{P} \otimes I_n)z_{\mathcal{T}}. \tag{19}$$

By taking the derivative of (19) along the trajectories of (17), we have

$$\begin{aligned} \dot{V}\left(z_{\mathcal{T}}\right) &= -z_{\mathcal{T}}^T(\mathcal{Q} \otimes I_n)z_{\mathcal{T}} + z_{\mathcal{T}}^T(\mathcal{P}\mathcal{L}_{\mathcal{T}1} \otimes I_n)\omega + \omega^T(\mathcal{L}_{\mathcal{T}1}^T\mathcal{P} \otimes I_n)z_{\mathcal{T}} \\ &\leq -\lambda_{\min}\left(\mathcal{Q}\right)\left|z_{\mathcal{T}}\right|^2 + 2\sqrt{2nL}\mu\Delta\left\|\mathcal{P}\mathcal{L}_{\mathcal{T}1}\right\|\left|z_{\mathcal{T}}\right| \\ &= -\left|z_{\mathcal{T}}\right|\lambda_{\min}\left(\mathcal{Q}\right)\left(\left|z_{\mathcal{T}}\right| - \Theta\mu\Delta\right) \end{aligned} \tag{20}$$

in which $\Theta = 2\sqrt{2nL}\left\|\mathcal{P}\mathcal{L}_{\mathcal{T}1}\right\|/\lambda_{\min}\left(\mathcal{Q}\right) > 0$.

Based on Lemma 1 of [20], for an arbitrary $\varepsilon > 0$, we can define the ellipsoids

$$R_1 := \left\{ z_{\mathcal{T}} : z_{\mathcal{T}}^T (\mathcal{P} \otimes I_n) z_{\mathcal{T}} \leq \lambda_{\min}(\mathcal{P}) \mathcal{M}^2 \mu^2 \right\}$$

and

$$R_2 := \left\{ z_{\mathcal{T}} : z_{\mathcal{T}}^T (\mathcal{P} \otimes I_n) z_{\mathcal{T}} \leq \lambda_{\max}(\mathcal{P}) \Theta^2 \Delta^2 (1+\varepsilon)^2 \mu^2 \right\}.$$

According to (20), R_1 and R_2 are invariant regions for multi-agent system (17). With this setting, the trajectories of (17) starting in R_1 will approach R_2 in finite time.

Between ellipsoids R_1 and R_2, we have the following formula:

$$\mathcal{M}\mu \geq |z_{\mathcal{T}}| \geq (1+\varepsilon)\Theta\mu\Delta$$

which implies

$$\dot{V} \leq -\lambda_{\min}(\mathcal{Q}) \frac{\varepsilon}{1+\varepsilon} |z_{\mathcal{T}}|^2 \leq -\frac{\lambda_{\min}(\mathcal{Q})}{\lambda_{\max}(\mathcal{P})} \frac{\varepsilon}{1+\varepsilon} V. \tag{21}$$

Let $\alpha = \lambda_{\min}(\mathcal{Q})\varepsilon/\lambda_{\max}(\mathcal{P})(1+\varepsilon)$, then by applying the Comparison Lemma [21], we can provide the following estimates of the convergence rate as in [12]:

$$V(z_{\mathcal{T}}(t)) \leq e^{-\alpha t} V(z_{\mathcal{T}}(0))$$

with the estimation of the upper bound of the convergence time that starting in R_1 enter R_2 as

$$T = \frac{1}{\alpha} \ln \frac{\lambda_{\min}(\mathcal{P}) \mathcal{M}^2}{\lambda_{\max}(\mathcal{P}) \theta^2 \Delta^2 (1+\varepsilon)^2}. \tag{22}$$

To guarantee the asymptotic stability of the whole system, the Liberzon's design strategy [20] is employed. The control scheme contains two steps: "zooming-out" to detect measurement of states by increasing μ; "zooming-in" to achieve more accurate quantization by decreasing μ.

Zooming-out. Firstly, we initialize $u_i = 0$ and let $\mu(0) = 1$. By increasing μ fast enough to dominate the rate of growth of $\left|e^{At}\right|$, then we can pick a time t_0 such that

$$\left| q_\mu (z_{\mathcal{T}}(t_0)) \right| \leq \sqrt{\frac{\lambda_{\min}(\mathcal{P})}{\lambda_{\max}(\mathcal{P})}} \mathcal{M}\mu(t_0) - \Delta\mu(t_0).$$

Therefore, we can obtain

$$\left| \frac{z_{\mathcal{T}}(t_0)}{\mu(t_0)} \right| \leq \sqrt{\frac{\lambda_{\min}(\mathcal{P})}{\lambda_{\max}(\mathcal{P})}} \mathcal{M}$$

which implies that $z_{\mathcal{T}}(t_0)$ belongs to the ellipsoid $R_1(\mu(t_0))$. This event can be detected by using only available quantized measurements.

Zooming-in. When the initial state is in ellipsoid R_1 with the initial zooming variable $\mu(t_0)$, the zooming-in phase starts with the update interval T. Let $\mu(t) = \mu(t_0)$ for $t \in [t_0, t_0 + T)$, where T is given by (22). Then $x(t_0 + T)$ belongs to the ellipsoid R_2. Let the zooming-in rule is as

$$\mu = \Omega^k \mu_0, \quad \Omega = \frac{\sqrt{\lambda_{\max}(\mathcal{P})}\Theta\Delta(1+\varepsilon)}{\sqrt{\lambda_{\min}(\mathcal{P})}\mathcal{M}} \tag{23}$$

for $t \in [kT, (k+1)T]$ where T is defined as (22) and k is the number of update times. According to (18), it is easy to check $\Omega < 1$ and $\mu(t_0 + T) < \mu(t_0)$. To decrease μ by means of multiplying it by the scaling factor Ω, we have $\mu(t) \to 0$ which also implies $z_{\mathcal{T}}(t) \to 0$.

Remark 1. With the quantization range $\mathcal{M}$, the quantizer obtains $(2\mathcal{M}+1)$ quantization levels. In addition, only $\lceil \log_2(2\mathcal{M}) \rceil$ bits are required while transmitting data at each time interval.

Remark 2. As the initial states of multi-agent system are generally known for quantizers, we can select a suitable zooming variable μ_0 in advance to keep the system starts in the ellipsoids R_1 without using the zooming-out stage.

4. Simulation

Consider the multi-agent system consisting of a group of five micro air vehicles associated with a quasi-strongly connected graph as shown in Fig. 3, where $e_1, e_2, e_3, e_4 \subset \mathcal{G}_{\mathcal{T}}$ and $e_5 \subset \mathcal{G}_{\mathcal{C}}$. Suppose the micro air vehicles work in indoor

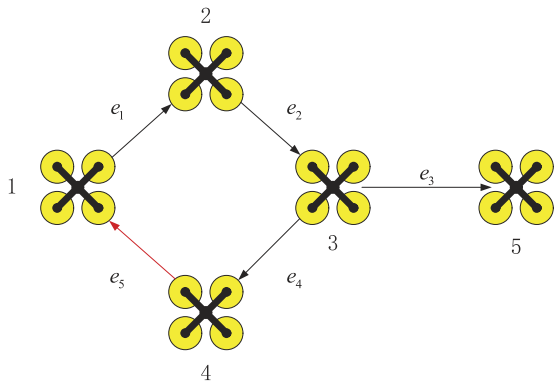

Fig. 3. A quasi-strongly connected graph of five micro air vehicles.

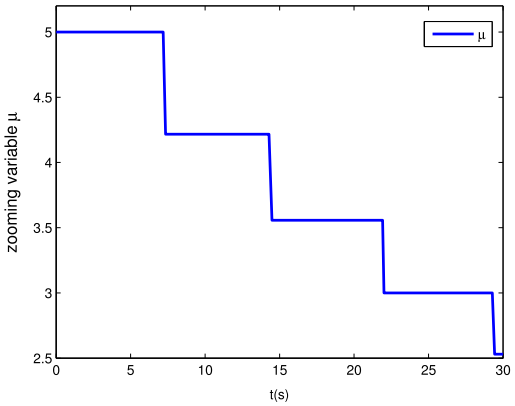

Fig. 4. The amplitude of the zooming variable μ.

environment and the relative position and posture of them are obtained through motion capture systems by quantized communication [22]. Then, we apply the hybrid feedback control law (12) to achieve altitude alignment among multiple micro air vehicles. The simplified equation of motion for altitude of the ith rotary-wing micro air vehicle can be represented by

$$\ddot{h}_i = k_{hi}\left(\dot{h}_c^i - \dot{h}_i\right), \tag{24}$$

where h_i is the altitude, $\dot{h}_c^i$ is the altitude command to low-level controllers and k_{hi} is the autopilot parameter [23]. By simply letting $x_i = h_i$, $v_i = \dot{h}_i$, this model can be represented by (11). Then the altitude command can be given by

$$\dot{h}_c^i = \dot{h}_i + (1/k_{hi})\, u_i. \tag{25}$$

Through a simple calculation, we can obtain

$$T = \begin{pmatrix} -1.00 \\ -1.00 \\ 0.00 \\ -1.00 \end{pmatrix}, \qquad R = \begin{pmatrix} 1.00 & 0.00 & 0.00 & 0.00 & -1.00 \\ 0.00 & 1.00 & 0.00 & 0.00 & -1.00 \\ 0.00 & 0.00 & 1.00 & 0.00 & 0.00 \\ 0.00 & 0.00 & 0.00 & 1.00 & -1.00 \end{pmatrix}.$$

Suppose that the weighted diagonal matrix is defined as $\mathcal{W} = \mathrm{diag}\{0.12, 0.24, 0.44, 0.43, 0.09\}$. By choosing $\sigma = 1.64$, we have

$$\hat{L}_e = \begin{pmatrix} 0.21 & 0.09 & 0.00 & 0.09 \\ -0.12 & 0.24 & 0.00 & 0.00 \\ 0.00 & -0.24 & 0.44 & 0.00 \\ 0.00 & -0.24 & 0.00 & 0.43 \end{pmatrix}$$

$$\hat{L}_{\mathcal{O}} = \begin{pmatrix} 0.12 & 0.00 & 0.00 & 0.00 & -0.09 \\ -0.12 & 0.24 & 0.00 & 0.00 & 0.00 \\ 0.00 & -0.24 & 0.44 & 0.00 & -0.00 \\ 0.00 & -0.24 & 0.00 & 0.43 & 0.00 \end{pmatrix}.$$

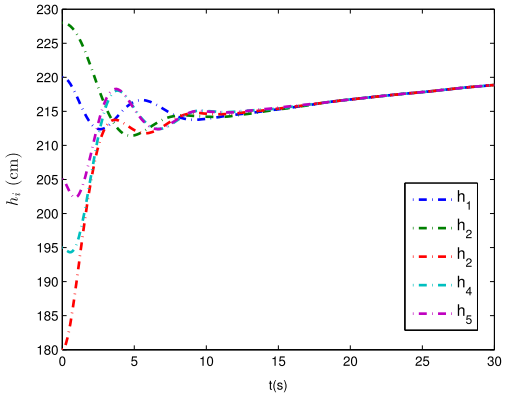

Fig. 5. Altitudes of each vehicle.

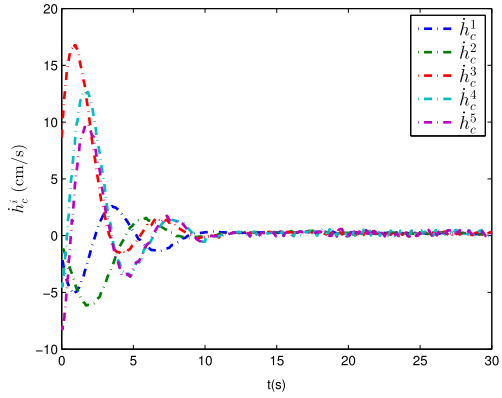

Fig. 6. Vertical velocities of each vehicle.

Solving the Lyapunov equation (10) leads to

$$H = \begin{pmatrix} 2.47 & 0.16 & 0.07 & -0.26 \\ 0.16 & 2.86 & 0.39 & 0.45 \\ 0.07 & 0.39 & 1.14 & -0.01 \\ -0.26 & 0.45 & -0.01 & 1.22 \end{pmatrix}.$$

Directed calculation yields $\lambda_{\max}(\mathcal{P}) = 8.098$, $\lambda_{\min}(\mathcal{P}) = 0.6157$, $\|\mathcal{P}\| = 8.098$ and $\|\mathcal{P}\mathcal{L}_{\mathcal{T}1}\| = 6.7121$.

Consider the quantized protocol (12) with the dynamic uniform quantizer (4). By choosing $\mathcal{M} = 63$ (i.e., only 7 bits information is required) with $\varepsilon = 0.75$, the condition (18) is satisfied. To ensure the initial condition lies in the ellipsoid R_1, μ_0 can be chosen to be 5. The resulted zooming interval of the scheme proposed in this paper is $T = 6.2597s$. The quantization error is assumed to be $\Delta = 0.2$. The change of the amplitude of the zooming variable is shown in Fig. 4. The achievement of the altitude alignment of the group of vehicles in Fig. 5 suggests that the hybrid feedback control law (12) works well. The vertical velocities are shown in Fig. 6. Finally, Figs. 7 and 8 show that the edge state $x_e(t)$ and $v_e(t)$ converge to the equilibrium points asymptotically.

5. Conclusion

In this paper, we explored the edge agreement problem of second-order multi-agent systems under quantized communication. Based upon the essential edge Laplacian, we proposed a model reduction representation of the closed-loop multi-agent system for directed graph. Then, the dynamic quantized communication strategy based on the zooming in-zooming out scheme with finite quantization level was proposed. By implementing the hybrid feedback law, the asymptotic stability of second-order multi-agent systems under dynamic quantized effects with only finite quantization level could be guaranteed.

Acknowledgment

This work was supported by the National Natural Science Foundation of China under grant 61403406.

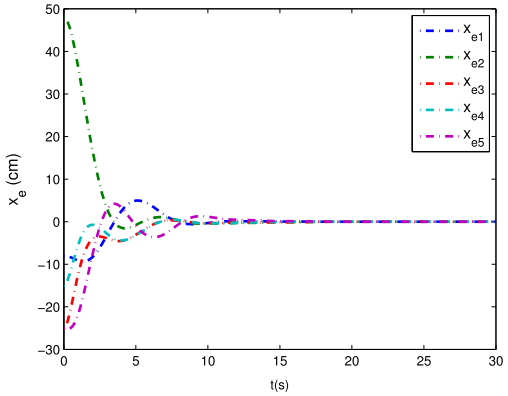

Fig. 7. Altitudes agreement $x_e \to 0$.

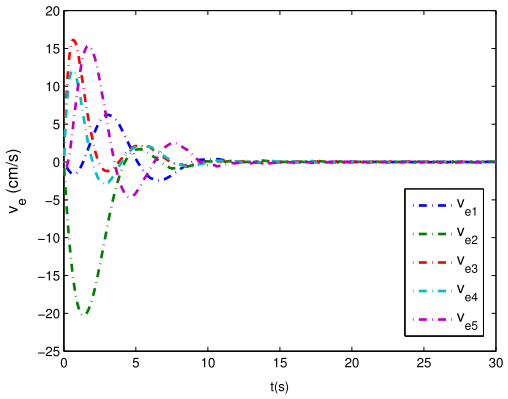

Fig. 8. Vertical velocities agreement $v_e \to 0$.

References

[1] R. Olfati-Saber, R.M. Murray, Consensus problems in networks of agents with switching topology and time-delays, IEEE Trans. Automat. Control 49 (9) (2004) 1520–1533.
[2] W. Ren, R.W. Beard, et al., Consensus seeking in multiagent systems under dynamically changing interaction topologies, IEEE Trans. Automat. Control 50 (5) (2005) 655–661.
[3] D.V. Dimarogonas, K.H. Johansson, Stability analysis for multi-agent systems using the incidence matrix: quantized communication and formation control, Automatica 46 (4) (2010) 695–700.
[4] J. Lavaei, R.M. Murray, Quantized consensus by means of gossip algorithm, IEEE Trans. Automat. Control 57 (1) (2012) 19–32.
[5] R. Carli, F. Bullo, S. Zampieri, Quantized average consensus via dynamic coding/decoding schemes, Internat. J. Robust Nonlinear Control 20 (2) (2010) 156–175.
[6] T. Li, M. Fu, L. Xie, J.-F. Zhang, Distributed consensus with limited communication data rate, IEEE Trans. Automat. Control 56 (2) (2011) 279–292.
[7] D. Li, Q. Liu, X. Wang, Z. Lin, Consensus seeking over directed networks with limited information communication, Automatica 49 (2) (2013) 610–618.
[8] D. Li, Q. Liu, X. Wang, Z. Yin, Quantized consensus over directed networks with switching topologies, Systems Control Lett. 65 (2014) 13–22.
[9] Q. Zhang, B.C. Wang, J.F. Zhang, Distributed dynamic consensus under quantized communication data, Internat. J. Robust Nonlinear Control 25 (11) (2015) 1704–1720.
[10] W. Yu, G. Chen, M. Cao, J. Kurths, Second-order consensus for multiagent systems with directed topologies and nonlinear dynamics, IEEE Trans. Syst. Man Cybern. B 40 (3) (2010) 881–891.
[11] T. Li, L. Xie, Distributed coordination of multi-agent systems with quantized-observer based encoding–decoding, IEEE Trans. Automat. Control 57 (12) (2012) 3023–3037.
[12] S. Yu, Y. Wang, L. Jin, K. Zheng, Asymptotic average consensus of continuous-time multi-agent systems with dynamically quantized communication, in: World Congress, Vol. 19, 2014, pp. 1819–1824.
[13] H. Liu, M. Cao, C. De Persis, Quantization effects on synchronized motion of teams of mobile agents with second-order dynamics, Systems Control Lett. 61 (12) (2012) 1157–1167.
[14] Z. Zeng, X. Wang, Z. Zheng, Edge agreement of multi-agent system with quantised measurements via the directed edge Laplacian, IET Control Theory Appl. (2016) http://dx.doi.org/10.1049/iet-cta.2015.1068.
[15] D. Zelazo, M. Mesbahi, Edge agreement: Graph-theoretic performance bounds and passivity analysis, IEEE Trans. Automat. Control 56 (3) (2011) 544–555.
[16] Z. Zeng, X. Wang, Z. Zheng, Convergence analysis using the edge laplacian: Robust consensus of nonlinear multi-agent systems via ISS method, Internat. J. Robust Nonlinear Control 26 (5) (2016) 1051–1072.
[17] K. Thulasiraman, M.N. Swamy, Graphs: Theory and Algorithms, John Wiley & Sons, 2011.
[18] D. Zelazo, S. Schuler, F. Allgöwer, Performance and design of cycles in consensus networks, Systems Control Lett. 62 (1) (2013) 85–96.
[19] J. Hu, Second-order event-triggered multi-agent consensus control, in: 2012 31st Chinese Control Conference, CCC, IEEE, 2012, pp. 6339–6344.
[20] D. Liberzon, Hybrid feedback stabilization of systems with quantized signals, Automatica 39 (9) (2003) 1543–1554.
[21] H.K. Khalil, J. Grizzle, Nonlinear Systems, Vol. 3, Prentice Hall, Upper Saddle River, 2002.
[22] D. Mellinger, M. Shomin, N. Michael, V. Kumar, Cooperative grasping and transport using multiple quadrotors, in: Distributed Autonomous Robotic Systems, Springer, 2013, pp. 545–558.
[23] W. Ren, E. Atkins, Second-order consensus protocols in multiple vehicle systems with local interactions, in: AIAA Guidance, Navigation, and Control Conference and Exhibit, 2005, pp. 15–18.